JOURNAL OF APPLIED ELECTROCHEMISTRY **26** (1996) 187–193

An electrochemical current efficiency model for aluminium electrolysis cells

Å. STERTEN

Department of Electrochemistry, The Norwegian Institute of Technology (NTH), The University of Trondheim, N-7034 Trondheim, Norway

P. A. SOLLI

Hydro Aluminium, Technology Centre Årdal, P.O. Box 303, N-5870 Øvre Årdal, Norway

Received 15 December 1994; revised 10 July 1995

Previous current efficiency models of the rate of aluminium production in Hall–Heroult cells are briefly summarized. A description and discussion of the cathode processes are given, and rate limiting steps are evaluated under the assumption of no concentration gradients in the bulk electrolyte phase during electrolysis. An electrochemical current efficiency model is derived from selected rate determining steps. The model expresses the local current efficiency in terms of the local partial current density for the aluminium deposition reaction and the local partial current density for all cathodic loss reactions. The model equations are valid both for laboratory and for commercial cells and independent of whether or not electrolyte impurities are involved in cyclic redox reactions. The necessary precautions to study the parameters affecting current efficiency both in commerical and in laboratory cells are outlined.

List of symbols

a_i	activity of component i in bulk of electrolyte
a_{i^*}	activity of component i at the interface
c_m	modified concentration of NaF, $c_m = (1.030 - 5.397 \times 10^{-4}T)(x_{NaF} - 0.35)^{0.445}$
D_i	diffusion coefficient of component i ($cm^2\,s^{-1}$)
F	Faraday constant ($C\,mol^{-1}$)
i_{Al}	local current density for the aluminium deposition reaction ($A\,cm^{-2}$)
i_{loss}	local current density for all cathodic side reactions ($A\,cm^{-2}$)
i_{sc}	local current density due to short circuits and dispersion of metal ($A\,cm^{-2}$)
i_c	local cathodic current density ($A\,cm^{-2}$)
J_i	local mass flux density of component i ($mol\,cm^{-2}\,s^{-1}$)
K_{add}	constant, Equation 25
k_i	local mass transfer coefficient for component i ($cm\,s^{-1}$)
k_{mix}	local mixed mass transfer coefficient (or standard rate constant) ($mol\,cm^{-2}\,s^{-1}$)
n_i	number of moles of component i in a given volume element ($mol\,cm^{-3}$)
V	integral molar volume ($cm^3\,mol^{-1}$)
wt % Add	weight percent additive to the $NaF–AlF_3$ melt
x	coordinate axis (cm)
x_i	molar fraction of component i (in the $NaF–AlF_3$ system)
y	empirical sodium activity exponent

Greek letters

α	Ratio between real sodium activity in bulk electrolyte and the corresponding activity when equilibrated with liquid Al of unit activity, $\alpha = (a_{Na,bulk})/(a_{Na,eq})$
ϵ	local current efficiency for the aluminium deposition reaction (%)
η	concentration overpotential/polarization (V)

1. Introduction

The main overall cell reaction in commercial aluminium electrolysis cells is

$$Al_2O_3 + \frac{3}{2}C = 2Al + \frac{3}{2}CO_2 \qquad (1)$$

Al_2O_3 is dissolved in liquid Na_3AlF_6 containing excess AlF_3, CaF_2 and in some cases MgF_2 and LiF. A consumable carbon anode liberates CO_2 with an anodic current efficiency close to 100%. The cathodic current efficiency (CE), referred to the production of aluminium, normally varies in the range 85–96% in commercial cells. Considerable work has been carried out in order to clarify the influence of various parameters on CE both in commercial and in laboratory cells. Literature reviews and surveys of results have been given by Grjotheim *et al.* [1, 2] and Kvande [3].

CE models are essentially of two main categories: (i) Empirical models based on measurements of CE in

0021-891X

commercial cells [4–6], and (ii) models based more or less on theory of mass transport coupled to electrochemical and chemical reactions [7–13]. In the following both empirical models and some theoretical models are briefly reviewed.

The present paper discusses primary and secondary overall electrode reactions, including mass transfer processes. It is proposed that electrolyte impurities are involved in cyclic redox reactions leading to loss in current efficiency with respect to aluminium. Rate limiting steps are isolated and used to develop a current efficiency model.

1.1. *Empirical models*

Berge *et al.* [4] have derived an empirical equation for CE as a function of temperature, excess AlF_3, metal height and cell age. The equation is based on CE measurements using radioactive gold tracer on 34 cells in a 135 kA line with prebaked anodes. The derived model equation is probably not generally valid for all types of commercial cells, but specific for the given cells design and operation.

Dewing [5] has derived an empirical equation for CE as a function of superheat, excess AlF_3, LiF and a constant term dependent on cell design. No effect of CaF_2 on CE was found. Dewing discussed probable mechanisms for the loss process and concluded, in agreement with previous work, that loss of CE most probably is controlled by mass transfer of dissolved metal in the cathode boundary layer.

Knapp [6] made a simple CE equation to predict the benefits achieved after a technical upgrade program carried out for two potlines. The parameters included in the CE equation are temperature, amperage and bath/metal interfacial area. The temperature of commercial cells is, of course, linked to bath chemistry, so that electrolyte composition is indirectly incorporated in the model. The model seems to be in reasonable agreement with observed changes in CE for the potlines in question.

CE models based on plant measurements and regression analysis may give good models for the cells in question and for the specific analysis period. Methods usually employed in such studies are short term analysis of anode gas composition (CO/CO_2), or by longer term time change of some metal phase tracer concentration. These methods all have their weaknesses when it comes to accuracy. In addition it is difficult in such studies to isolate certain variables like current density and mass transfer coefficients, believed to be important parameters in the derivation of a more generally valid CE model.

1.2. *Theoretical models*

Robl *et al.* [7] presented a rather general model for the loss or recombination process in which CE was directly calculated in terms of geometrical and operating factors such as anode-to-metal spacing, electrolyte temperature and composition. It was claimed that hydrodynamic parameters supply the 'missing link' which can explain the large range of correlation data reported in the literature. Haupin [14] has discussed the model equations in some detail.

Lillebuen *et al.* [8] described the rate of metal loss in terms of mass transport theory assuming the rate determining step to be dissolution of 'aluminium'. The process model is based on reaction between dissolved 'aluminium' and dissolved carbon dioxide. The model predicts changes in CE for variations in metal/electrolyte interfacial area, interelectrode distance, 'metal' solubility and interfacial velocity. The model is based on the assumption of a first order dependence of the CE loss with 'metal' solubility, expressed as a weight percentage of aluminium.

Peterson and Wang [9] coupled results from the metal solubility study of Wang *et al.* [15] with the model of Lillebuen *et al.* [8] to predict CE for some industrial cells. The study indicated that NaF/AlF_3 ratio and bath temperature are major variables influencing cell current efficiency. Peterson and Wang [9] calculated a dependence of CE on ratio at constant superheat of roughly −2.3% per 0.1 increase in NaF/AlF_3 molar ratio, which is three times higher than reported by Dewing [5] and Burck and Fern [16] under similar conditions in commercial cells. The temperature dependence of CE calculated by Peterson and Wang is roughly 50% higher than reported in the review given by Kvande [3]. The main reason for these large discrepancies is that the aluminium solubility data [15] applied by Peterson and Wang increase considerably more with temperature and NaF/AlF_3 ratio than corresponding solubility data from other sources [17–19].

Evans *et al.* [10] assumed the rate determining step in the loss process to be transport of dissolved metal through a concentration boundary layer at the metal/electrolyte interface. The equation for the rate of mass transfer includes the diffusion coefficient of dissolved metal, the bath density, the bath/metal surface tension, the turbulent kinetic energy due to the electromagnetic force field, the aluminium surface area and the solubility limit of dissolved 'metal'. The model does not account for the effect of possible gas induced turbulence in the bath.

Haarberg *et al.* [11, 12] have derived equations describing the influence of electronic conductivity on CE. For a cathode boundary layer thickness in the range 0.01 to 0.1 cm the calculated loss in CE amounted to about 7% in a melt consisting of Na_3AlF_6 saturated with alumina at 1000 °C [11]. The calculated loss in CE ranged from 2% to about 15% at 1000 °C for various specified conditions [12], indicating that the greater part of the loss in CE of commercial cells can be related to electronic conductivity.

Sterten [13] presented a model where the local current efficiency, ϵ, was defined by the following equation:

$$\epsilon = \frac{100 i_{Al}}{(i_{Al} + i_{loss} + i_{so})} \qquad (2)$$

where i_{Al} is the local partial current density of aluminium deposition, and i_{loss} is the local partial current density of all cathodic side reactions, while i_{sc} represents other losses due to local short circuits, dispersion of metal, etc. The sum $(i_{Al} + i_{loss} + i_{sc})$ is, by definition, equal to the local cathodic current density, i_c. The partial current densities, i_{Al} and i_{loss}, were modelled, the result being discussed below.

Current efficiency depends strongly on the cathode current density [13, 20, 21]. In fact, CE approaches zero and becomes negative [13, 22] when the current density approaches zero. The reason is that the rate of the aluminium deposition reaction decreases to lower values than the rate of the aluminium dissolution reaction or the rate of formation of dissolved 'metal'. This is in agreement with the fact that there is a continuous loss of aluminium from the metal phase when exposed to a cryolitic melt in a laboratory cell, and zero current. The local cathodic current density and, hence, CE are a function of time and space in commercial cells, related to cell operations like anode replacement, alumina feed procedures and other transient changes in electrolyte temperature and composition.

An apparent weakness of most of the models discussed above is that the influence of the cathodic current density on CE is not included. Some of the models [7–10] have a fixed equilibrium concentration of dissolved 'aluminium' independent of current density included in the model equations. As discussed below, this is an oversimplification which my lead to serious errors in calculated values for CE. The mass transfer coefficient introduced into the model equations is usually referred to weight percentage of dissolved 'aluminium' as the concentration measure. The coefficient defined this way may exhibit a considerable melt composition dependence.

A sound basis for developing a CE model for aluminium electrolysis cells is a detailed understanding and description of the cathode processes, including rate limiting steps both for the aluminium production process and for parallel processes giving rise to loss of CE. Such a description was given in a recent paper [23]. A short summary of the main process steps is reviewed below as a basis for the development of model equations.

2. The cathode processes and rate limiting steps

It is assumed that there are negligible concentration gradients in the bulk of the electrolyte phase. An impurity level of the same order of magnitude as in commercial aluminium electrolysis cells is assumed in the electrolyte phase.

2.1. *Main cathode process*

The overall main cathode process at current densities of industrial importance may be separated into three steps [23]:

(i) Mass transport of AlF_3 to the cathode (aluminium) interface.
(ii) The main overall electrode reaction,

$$AlF_3 + 3Na^+ + 3e^- = Al + 3NaF \qquad (3)$$

(iii) Mass transport of NaF away from the cathode interface. ($3Na^+$ can be considered to be approximately the charge transferred.)

The rate limiting steps for this cathode process are the mass transport of AlF_3 and of NaF in the cathode boundary layer giving rise to a cathodic concentration polarization [13].

2.2. *Loss process: reactions, mass transfer and rate limiting steps*

The following steps are proposed for the loss process [23]:

(iv) Cathode side reactions forming reduced entities (RE), both monovalent aluminium (AlF_2^-),

$$\frac{1}{2}Na^+ + \frac{1}{2}AlF_3 + e^- = \frac{1}{2}AlF_2^- + \frac{1}{2}NaF \qquad (4)$$

and sodium dissolved in the electrolyte phase,

$$Na^+ + e^- = Na \qquad (5)$$

Dissolved sodium is, from a structural point of view, related mainly to localized electrons in the cathode boundary layer of the electrolyte phase, the formation of which may tentatively be written [23],

$$e^- = e' \qquad (6)$$

(v) Corresponding main primary anode reaction,

$$\frac{1}{2}O^{2-} + \frac{1}{4}C = \frac{1}{4}CO_2 + e^- \qquad (7)$$

(vi) Mass transport of RE from the cathode (metal) surface to a reaction plane A located inside the cathodic diffusion layer.
(vii) Mass transport of reducible impurities from the electrolyte bulk phase towards the reaction plane A.
(viii) Reactions between impurities and RE in plane A, exemplified by

$$Fe^{3+} + e' = Fe^{2+} \qquad (8)$$

(ix) Mass transport of reduced impurity species both towards the cathode where they are reduced to the metallic state, and towards the bulk of the electrolyte.
(x) Convective mass transport of reduced impurity species through the bulk phase to the anode boundary layer.
(xi) Diffusive transport of reduced impurity species in the anode gas boundary layer to reaction site B in the anode/anode gas boundary layer.
(xii) Equilibrium reactions between impurities and dissolved anode gases in site B, for example,

$$Fe^{2+} + \frac{1}{2}CO_2 = Fe^{3+} + \frac{1}{2}CO + \frac{1}{2}O^{2-} \qquad (9)$$

(xiii) Mass transport of oxidized impurities (like Fe^{3+}) from site B towards the bulk electrolyte phase, where they are involved in a new cycle, step (vii).

Combination of an arbitrary cathodic side reaction in step (iv) with all other steps from (v) to (xiii) gives *the overall loss process*, corresponding to a consumption of 1 F,

$$\frac{1}{4}CO_2 + \frac{1}{4}C = \frac{1}{2}CO \qquad (10)$$

When considering the loss process, as for any chemical or electrochemical process, only rate determining steps are suitable for modelling. In commercial Hall–Heroult cells, with rapid convective mass transport in the electrolyte phase, the mass transport steps (vi) and (vii) in the cathode boundary layer are assumed to be the most important rate limiting steps in the loss process. Steps (vii), (ix), (xi) and (xiii), involving cyclic diffusion of impurities in the boundary layers, will, of course, influence the flux of dissolved metal species away from the cathode and, as such, be partly rate determining for the loss process [23].

Occasionally, the impurity distribution in commercial cells may locally, or generally, depart from the description given in the reaction sequence above. Under certain circumstances it is believed that the bulk electrolyte phase may contain RE, and that the impurities present are either reduced to low equilibrium concentrations or to a metallic state [23]. This reaction scheme is in agreement with the presently accepted way of expressing the 'back reaction', in the sense that RE are considered to be transported to the gas/electrolyte interface before being oxidized either by the anode or by the anode gases. The rate limiting step suited for modelling is, also in this case, mass transport of RE through the cathode boundary layer.

3. Current efficiency model

It follows from the above discussion that it is desirable to carry out an electrochemical modelling of the main and secondary cathode reactions. Hence the local partial cathode current density and the local electrode overvoltage will be important parameters in the derivation of model equations. Equation 2 is therefore adopted as an equation defining CE.

3.1. *Modelling of the main reaction*

As discussed above the rate limiting steps for the primary cathode process are mass transport of NaF and AlF_3 in the cathode boundary layer. The flux densities are interlinked by the following equation,

$$J_{NaF} = -3J_{AlF_3} \qquad (11)$$

which is approximately valid under steady state conditions. The partial current density for aluminium deposition may, thus, be written:

$$i_{Al} = FJ_{NaF} = -3FJ_{AlF_3} \qquad (12)$$

The flux density equation for NaF in the binary non ideal NaF–AlF_3 system, can be expressed by the following equation [13],

$$J_{NaF} = -D_{NaF}\frac{x_{NaF}}{V}\left[\frac{d\ln a_{NaF}}{dx}\right]_{x=0} \qquad (13)$$

where D_{NaF} is the diffusion coefficient of NaF, a_{NaF} is the activity referred to pure liquid NaF as the standard state, and x_{NaF} is the molar fraction of NaF in the binary NaF–AlF_3 system, given by,

$$x_{NaF} = \frac{n_{NaF}}{n_{NaF} + n_{AlF_3}} \qquad (14)$$

where n is the number of moles of NaF and AlF_3 in a given volume element. V in Equation 13 is the corresponding integral molar volume, and x denotes the coordinate axes directed normally from the metal surface into the melt. The concentration overvoltage, η, related to the rate limiting steps for the aluminium deposition Reaction 3, can be expressed by,

$$\eta = \frac{RT}{F}\ln\frac{a_{NaF}}{a_{NaF^*}} + \frac{RT}{3F}\ln\frac{a_{AlF_3^*}}{a_{AlF_3}} \qquad (15)$$

The asterisks (*) denote activities at the aluminium/melt interface, with solid AlF_3 as the standard state for dissolved AlF_3.

Sterten [13] combined the Equations 12 to 15 in an empirical manner and arrived at the following equation for the rate of aluminium deposition,

$$i_{Al} = Fk_{NaF}c_m[-1 + \exp(-0.605\eta)] \qquad (16)$$

where k_{NaF} is the mass transfer coefficient for NaF in the cathode boundary layer and c_m (mol cm^{-3}) is a modified concentration of NaF given by

$$c_m = (1.030 - 5.397 \times 10^{-4}T)(x_{NaF} - 0.35)^{0.445} \qquad (17)$$

which reflects the variations in the 'effective' NaF-concentration when the electrolyte composition is changed.

Equation 16 and 17 are strictly valid only for NaF–AlF_3 melts. This means that increasing concentrations of additives like Al_2O_3 and CaF_2 may give increasing errors in c_m, the magnitude of which needs to be checked experimentally.

3.2. *Modelling of the loss process*

The electrochemical side Reactions 4, 5 and 6 and the subsequent rate limiting step (vi) discussed above are used to model the loss process. However, at present it is impossible to determine all individual current densities of reduced species (AlF_2^-, Na and or e′) in the cathode boundary layer. The individual gradients of the reduced entities are interlinked by internal homogeneous equilibria such as

$$2Na + AlF_3 = NaAlF_2 + NaF \qquad (18)$$

and equilibria involving dissolved Na and e′. The true nature of e′ cannot be accurately specified, but the concentration must be a function of the sodium

activity. This means that all reduced entities establish concentration profiles in the cathode boundary layer interlinked to the sodium activity profile. The partial current density of all side reactions, i_{loss}, may, therefore, tentatively be described by the empirical relationship,

$$i_{loss} = Fk_{mix}(a^{y}_{Na^*} - a^{y}_{Na,bulk}) \quad (19)$$

where the activity terms reflect an overall driving force for the loss process. k_{mix} is a mixed mass transfer coefficient (or a mixed standard rate constant) defined by this equation. The coefficient may be roughly independent of melt composition, although this needs to be experimentally clarified. The exponent y may depend on melt composition and the numerical value is not easily predicted from theoretical considerations. This means that y, as a function of melt composition, needs to be experimentally determined. Equation 19 is generally valid, in the sense that the bulk phase may contain RE, giving rise to a certain activity of sodium in the bulk phase, $a_{Na,bulk}$. This activity may be related to the fraction, α, as follows:

$$\alpha = \frac{a_{Na,bulk}}{a_{Na,eq}} \quad (20)$$

where the equilibrium activity, $a_{Na,eq}$, can be computed from the equilibrium constant for the reaction,

$$3NaF + Al = AlF_3 + 3Na \quad (21)$$

with bulk phase activities of NaF and AlF_3 and a hypothetical unit activity of Al.

Equation 15, describing concentration overvoltage for the aluminium deposition Reaction 3, may be combined with the expression for the equilibrium constant for Reaction 21, yielding the following relationship between sodium activities and overvoltage,

$$\eta_{Al} = \frac{RT}{F}\ln\left[\frac{a_{Na,eq}}{a_{Na^*}}\right] \quad (22)$$

Combination of Equations 19, 20 and 22 gives

$$i_{loss} = Fk_{mix}a^{y}_{Na,eq}\left[-\alpha^{y} + \exp\left(\frac{-F\eta y}{RT}\right)\right] \quad (23)$$

as the basic equation for current loss in aluminium electrolysis cells. It should be emphasised that the influence of e′ on current loss is included in Equation 23.

3.3 *Activity of sodium in the electrolyte*

From activity data for NaF and AlF_3 [24] and values for the standard Gibbs energy change [25] for Reaction 21, the equilibrium activity of sodium, $a_{Na,eq}$, may be calculated as a function of the temperature and the mole fraction of NaF in the binary NaF–AlF_3 system. The calculated activities of sodium, with a standard state pressure of 1 bar, were fitted to the following empirical equation,

$$a_{Na,eq}(\text{binary}) = \exp\left[50.633 + \frac{(-50\,498 + 44\,000\,x_{NaF})}{T} - \frac{(9.9 + 35\,x^2_{NaF})}{x_{NaF}}\right] \quad (24)$$

valid in the temperature range from the liquidus surface of the system and to about 1300 K.

The points in Fig. 1 show calculated activities of sodium as a function of NaF/AlF_3 molar ratio for three different temperatures, in good agreement with the full drawn lines from Equation 24.

Other components in the electrolyte will have the effect of altering the equilibrium activity of sodium, either through acid/base behaviour of the third component, or through a purely dilutive effect. The activity of sodium in a system containing one or more components in addition to NaF and AlF_3, may tentatively and approximately be described by the empirical relation,

$$a_{Na,eq} = a_{Na,eq}(\text{binary}) \times \exp\left[\sum\left(\frac{\text{wt \% Add}}{K_{Add}}\right)\right] \quad (25)$$

where the term $a_{Na,eq}$(binary) can be calculated from Equation 24. K_{Add} is assumed to be a constant characteristic of the influence of the additive (wt % Add) on the activity of sodium. The activity was derived as a function of alumina concentration using the activity data of Sterten and Mæland [24], while the activity as a function of the concentration of CaF_2 was derived from data given by Ødegård [26]. The

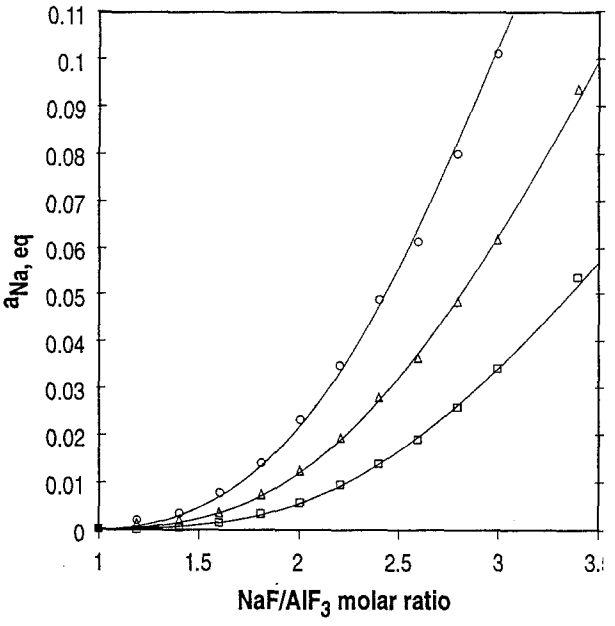

Fig. 1. Calculated equilibrium activities of sodium at 1200, 1253 and 1300 K as a function of the NaF/AlF_3 molar ratio, in the NaF–AlF_3–Al system. Points: activities from thermodynamic data [24, 25]. Lines: activities from Equation 24 (see text). Temperatures: (□) 1200, (△) 1253 and (○) 1300 K.

following empirical relationship was found for the equilibrium activity of sodium:

$$a_{Na,eq} = a_{Na,eq}(\text{binary}) \times \exp\left[-\frac{\text{wt \% } CaF_2}{19} + \frac{\text{wt \% } Al_2O_3}{85}\right] \quad (26)$$

Equation 26 can be expanded to include the influence of other species (LiF, MgF_2 etc.) on the equilibrium activity of sodium. However, the empirical and uncertain nature of Equation 26 must be emphasized. When improved thermodynamic data are available it may be necessary to include concentration cross terms in this equation in order to achieve a satisfactory thermodynamic description of the multicomponent system.

4. Discussion and applications of model equations

Equations 2, 16, 20 and 23 constitute the general CE model, while 14, 17, 24 and 26 are empirical equations developed to perform parameter studies based on data from laboratory and commercial cells.

4.1. *Commercial cells*

It follows from the above discussion and equations, that the *local* CE, ϵ, is a function of various parameters as indicated by the equation,

$$\epsilon = f(i_{Al}, i_{loss}) = f(x_{NaF}, x_{AlF_3}, x_1, x_2, \ldots, x_n, T, k_{NaF}, k_{mix}, \eta) \quad (27)$$

where $x_1, x_2, \ldots, x_n$ are wt% additives including impurities. The parameters k_{NaF}, k_{mix} and η vary somewhat from one region to another on the metal surface in commercial cells, especially in Søderberg cells, depending on the local cathodic current density and the local dynamic flow originating from the gas induced and magneto induced forces in the cells.

In commercial, as well as laboratory, cells it is often reasonable to assume that α is zero, i.e. that the concentration of dissolved metal in the bulk of the electrolyte approaches zero. This assumption simplifies the model equations. However, since there are considerable variations in the cathodic current density, especially in Søderberg cells it is necessary to evaluate at least one of the following integrals at a given time,

$$I_{Al} = \int_0^A i_{Al}\, dA \quad (28)$$

$$I_{loss} = \int_0^A i_{loss}\, dA \quad (29)$$

in order to evaluate the overall cell current efficiency. The sum $I_{Al} + I_{loss}$ represents the total cell current if there are no short circuits in the cell. A further treatment of the equations must await an experimental elucidation of how the parameters k_{NaF}, k_{mix} and η are interlinked with the partial current densities and the dynamic flow in the cells.

It may be difficult to estimate numerical values for i_{sc} (see Equation 2) in commercial cells. The term may probably attain a nearly constant value during stable operation of a given cell.

4.2. *Laboratory cells with even current distribution*

The CE model should be studied in a laboratory cell giving a constant and evenly distributed cathodic current density, i_c. Equation 2 may then be rewritten to yield ($i_{sc} = 0$),

$$\epsilon = \frac{100\,(i_c - i_{loss})}{i_c} \quad (30)$$

By establishing the relationship between i_c and η in the cell, and by measuring CE as a function of temperature and melt composition, it is possible under certain assumption to work out all parameters in the model equations. In fact CE as a function of individual variable parameters like cathodic current density, temperature, NaF/AlF_3 ratio, Al_2O_3 concentration and CaF_2 concentration and certain impurity concentrations has been studied in a specially designed laboratory cell. Results from these investigations will be published in the near future.

Acknowledgements

Financial support from The Research Council of Norway and from Norwegian aluminium industry is gratefully acknowledged. The work is performed in cooperation with Electrolysis Group, SINTEF Materials Technology.

References

[1] K. Grjotheim, C. Krohn, M. Malinovsky, K. Matiasovsky and J. Thonstad, 'Aluminium Electrolysis. Fundamentals of the Hall–Heroult process', 2nd edn, Aluminium-Verlag, Düsseldorf (1982).
[2] K. Grjotheim, W. E. Haupin and B. J. Welch, Light Metals (edited by H. O. Bohner), Proceedings of the 114th TMS annual meeting (1985), p. 679.
[3] H. Kvande, 'Light Metals' (edited by P. G. Campbell), Proceedings of the 118th TMS annual meeting (1989), p. 261.
[4] B. Berge, K. Grjotheim, C. Krohn, R. Næumann and K. Tørklep, 'Light Metals', Proceedings of the 104th TMS annual meeting (1975), p. 37.
[5] E. W. Dewing, *Met. Trans.* **22B** (1991) 177.
[6] L. L. Knapp, Light Metals (edited by E. R. Cutshall), Proceedings of the 121st TMS annual meeting (1992), p. 537.
[7] R. F. Robl, E. W. Haupin and D. Sharma, 'Light Metals' (edited by K. B. Higbie), Proceedings of the 106th TMS annual meeting (1977), p. 185.
[8] Lillebuen, S. A. Ytterdahl, R. Huglen and K. A. Paulsen, *Electrochim. Acta* **25** (1980) 131.
[9] R. D. Peterson and X. Wang, 'Light Metals' (edited by E. L. Rooy), Proceedings of the 120th TMS annual meeting (1991), p. 331.
[10] J. W. Evans, Y. Zundelevich and D. Sharma, *Met. Trans.* **12B** (1981) 353.
[11] G. M. Haarberg, K. S. Osen, J. Thonstad, R. J. Heus and J. Egan, Light Metals (edited by E. L. Rooy), Proceedings of the 120th TMS annual meeting (1991), p. 283.
[12] G. M. Haarberg, K. S. Osen, J. Thonstad, R. J. Heus and J. Egan, *Met. Trans.* **24B** (1993) 729.
[13] Å. Sterten, *J. Appl. Electrochem.* **18** (1988) 473.
[14] E. W. Haupin, *in* 'Production of Aluminium and Alumina' (edited by A. R. Burkin), John Wiley, New York (1987) chapter 8.

[15] X. Wang, R. D. Peterson and N. Richards, 'Light Metals' (edited by E. L. Rooy), Proceedings of the 120th TMS annual meeting (1991), p. 323.
[16] J. W. Burck and D. Fern, 'Light Metals' (edited by T. G. Edgeworth), Proceedings of the 100th TMS annual meeting (1971), p. 123.
[17] J. Thonstad, *Can. J. Chem.* **43** (1965) 3429.
[18] K. Yoshida and E. W. Dewing, *Met. Trans.* **3** (1972) 1817.
[19] R. Ødegård, Å. Sterten and J. Thonstad, *ibid* **19B** (1988) 449.
[20] S. Gjerstad and N. E. Richards, *J. Electrochem. Soc.* **113** (1966) 331.
[21] P. Å. Solli, T. Haarberg, T. Eggen, E. Skybakmoen and Å. Sterten, 'Light Metals' (edited by U. Mannweiler), Proceedings of the 123rd TMS annual meeting (1994), p. 195.
[22] Å. Sterten, 'Light Metals' (edited by E. L. Rooy), Proceedings of the 120th TMS annual meeting (1991), p. 445.
[23] Å. Sterten and P. Solli, *J. Appl. Electrochem.* **25** (1995) 809.
[24] Å. Sterten and I. Mæland, *Acta Chem. Scand.* **A39** (1985) 241.
[25] M. W. Chase, C. A. Davies, J. R. Downey, D. J. Frurip, R. A. McDonald and A. N. Syverud, 'JANAF Thermochemical Tables', 3rd. edn, *J. Phys. Chem. Data* **14**, Suppl. 1 (1985).
[26] R. Ødegård, 'Solubility and Electrochemical Behaviour of Al and Al_4C_3 in Cryolitic Melts', Thesis, Norwegian Institute of Technology, Trondheim, Norway (1986).